

# Modeling and analysis of the effective parameters on the heat transfer systems in the combustion chamber of engines with liquid fuel

**Ali Heidari**

Master of Mechanical Engineering, South Tehran Branch, Islamic Azad University, Tehran, Iran.  
Aliheidarii1995@gmail.com

## **Abstract:**

Due to high efficiency and lack of contaminants resulting from cryogenic engines combustion as well as high energy content of these motors they are increasing used for space shuttle engines. So, this clarifies the necessity of more analysis of these fuels besides improving the efficiency of internal combustion engines. Prediction of transport phenomena in liquid rocket engines because of some complexities was impossible to be done, but today it happens via using the simulation software. The present research is an attempt to examine the results of modeling and simulation of flow field and the temperature inside the combustion chamber with liquid fuel applying the combustion models in combination with the turbulence models. The simulation results and turbulence model predicted well the temperature inside the combustion chamber. Also, with regard to the simulation results of the combustion chamber, the effects of change of geometric parameters of the cooling ducts on transfer of the engine thrust chamber with liquid fuel. These geometrical parameters include number and frequency of the cooling channels height, fins thickness and the inner wall of the drift chamber. The results indicate that with decrease of flowing cross section of refrigerants from the channel and reduction of the thickness of the inner wall chamber, the wall temperature will also reduce. As the maximum wall temperature occurs in the throat area, increasing the number of cooling channels has a direct impact on the reduction of the maximum wall temperature, but with increase of the height, the maximum wall temperature will increase.

**Keywords:** combustion gas flow, cooling channels, modeling and simulation of heat transfer, liquid fuel engine

## **Introduction:**

Special efficiency and the absence of emissions from the combustion of hydrogen cryogenic propellant and high energy content of the propellant have created very good prospects for the use of this fuel in spacecraft engines. Main engine of space shuttle is among this type of engine uses this fuel (Gutheil, 2001). Therefore, improving the efficiency of internal combustion engines is one of the main issues for combustion science researchers. So, knowledge of the nature of the flow and combustion inside combustion chamber of internal combustion engines to improve their performance is very important (Dinler & Yucel, 2007).

Most rocket engines are of internal combustion type (Reddy et al., 2011). Prediction of transfer phenomena inside liquid rocket engine due to the complexity of many of the conditions in the combustion chamber have not been possible so far (Masquelet, 2006). In the liquid fuel engine, in order to protect interior wall of the chamber against hot gases caused from the combustion, one of the propellant after passing through the cooling channel wall, is injected into the combustion chamber. Flows into the combustion chamber is mainly of turbulence flows and for analysis of the flow parameters it is needed for modeling turbulent combustion flows. Prediction of heat transfer characteristics in the drift chamber is very important for

designing liquid fuel engine with retrieval cooling highly matters. Reducing the wall temperature of the hot gases at about 50 to 100 ° C caused a two-fold increase of chamber life is important in the space missions industry due to the high cost of production.

The necessity to enhance the performance of high-pressure combustion devices in liquid-propellant rockets requires high chamber pressures. In a liquid rocket engine thrust chamber, higher chamber pressures allow a higher specific impulse for the engine to be produced. Liquid fuels and/or oxidizers are usually delivered to combustion chambers as a spray of droplets, which then undergo a sequence of vaporization, mixing, ignition, and combustion processes at pressure levels well above the thermodynamic critical points of the fluid. Near the critical point, reactants properties show liquid-like densities, gas-like diffusivities, and pressure-dependent solubility.

Several studies on analysis of heat transfer in liquid-fueled engine drift chamber have been done. Marchi et al (2004) presented a one-dimensional mathematical model for the non-combustible gas in the drift chamber with retrieval cooling. The model is obtained with coupled equations of gas flow in the chamber, the fluid flow in cooling channels and thermal conductivity of the wall. Numerical study of film and retrieval cooling in the drift chamber was performed by Zhang et al (2007). Exchange of heat and mass transfer between the hot gas stream and a liquid thin film inside the chamber with a two-dimensional non-combustible gas flow model and for fluid flow cooling in the channel, a one-dimensional model is used.

A 3D model for the numerical simulation of fluid flow in cooling channel of liquid rocket motor drift chamber is provided by Wang et al (2006). They found approximately 335 optimal channels with an acceptable pressure drop in the channel. A 2D mathematical model of combustible gas flow in the nozzle of the liquid fuel engine was presented by Cai et al (2007) and VanOverbeke and Shuen (1989). In this model, radiations effects of gases and retrieval cooling are not considered. Hence, this study aims to model turbulent combustion flow of liquid fuel combustion chamber with the aid of fluid simulation software and temperature parameters inside the chamber with the existing turbulence model.

Combustion chamber of advanced rocket uses a liquid oxidizer which, is injected in higher than the critical temperature and pressure into the combustion chamber. Therefore, the surface tension of drops tends to zero, and the droplets get unstable. Because of that, the distance between the liquid and gas phases disappears, the flow can be considered as a homogeneous phase.

Therefore, the Eulerian method flow formula can be used to model the combustion (Benarous, et al., 2007). A one-dimensional mathematical model has been provided to simulate the gas flow in the chamber, the flow pass through cooling channels and thermal conductivity of the wall which, the effects of cross-sectional area of flow, friction, heat transfer and chemical reactions and gases radiations into the wall are considered.

In the past the research Mayer and Tamura (1996), Candel et al., (1998), Smith et al., (2002) has concerned the cryogenic propellant combustion under subcritical and transcritical conditions, in particular in the case of liquid oxygen and gaseous hydrogen injected from a single element at various chamber pressures (0.1–7 MPa). Recently, there is a great interest in the development of reusable liquid rocket engines operating with methane and oxygen as propellants. Extensive efforts have been made in experimental works to characterize the dynamics of supercritical fluid injection and mixing Chehroudi et al., (2002), Oschwald and Schik, (1999), Mayer et al., (2003) and Oschwald et al., (2006).

### **Modeling method:**

Figures 1 to 3, illustrate the study engine, type of cryogenics coaxial injector fuel injection, and cooling channel geometry respectively. The used fuel is hydrogen and a type of liquid and liquid oxygen oxidizer and the type of combustion is non-premixed combustion. The fuel injection site is on the central axis of the input current. In the study conditions, oxygen at a pressure of 60 bar and a temperature of 100k, speed 4.35m / s and 298k and hydrogen at temperature 298k and speed 168m / s entered into the combustion chamber. In the present study, water is used as a refrigerant in the channels. The chamber pressure was determined 20bar, and

input temperature and fluid mass flow rate of cooling were specified respectively 300k, and 20kg /s and the inner wall was made of copper.

To solve the two-dimensional and axial symmetric flow field, a numerical code is increased with turbulence models was used. In this numerical code, the governing equations were dismissed and were performed via volume control method using the simple algorithm. In the location of the flow input speed, boundary condition is input pace and walls in form of constant temperature at 1200k. At the walls place, non-slip boundary condition at the wall using standard wall functions was included. In addition to the above components, the radial velocity and zero gradient for the dependent variables, of the flow were applied as the boundary condition in symmetry axis.

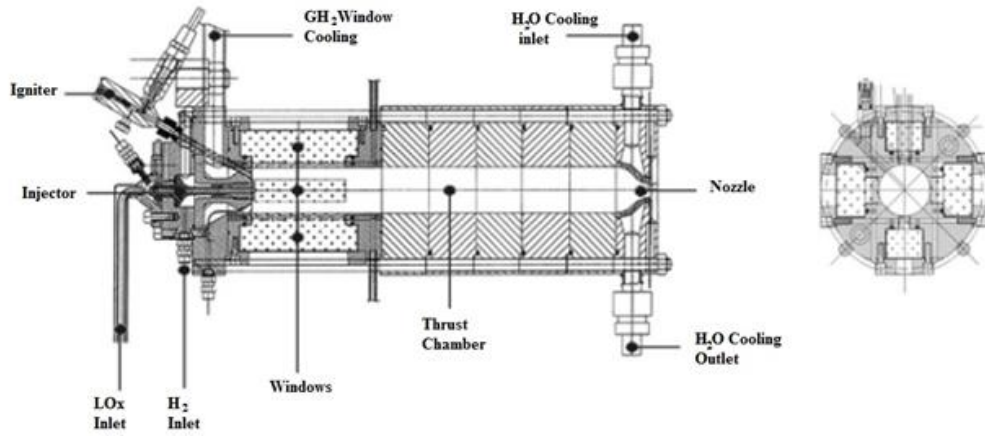


Fig.1: fluid fuel engine with cryogenic (H2-O2)

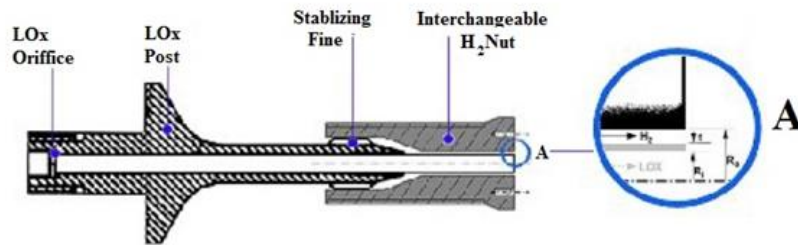


Fig.2: cut in single component with a coaxial geometry change

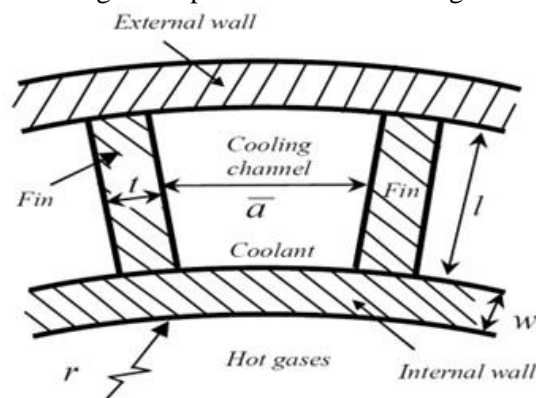


Fig.3: the geometry of cooling channel

Fig. 4 illustrates adiabatic flame temperature close to 3500k which mixing fraction (7.5 to 8.0) temperature of the combustion flame appears. Due to the high difference occurs in fluid mixture it is better to take transitional properties of a varying temperature.

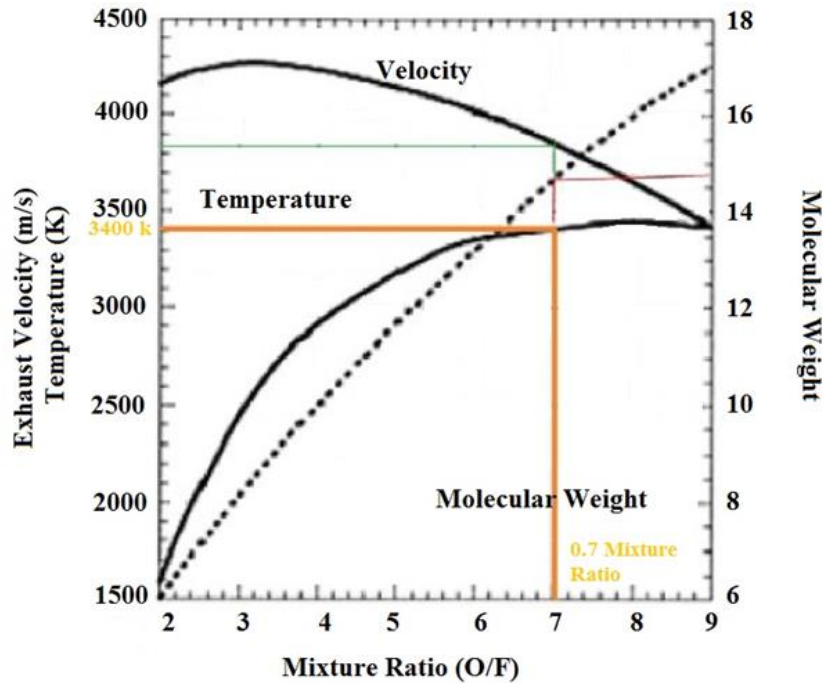


Fig.4: ratio of speed-temperature-molecular weight to mixing fraction of hydrogen-oxygen fuel

$$\lambda(T) = \sum_{i=0}^4 \alpha_i T^i \quad , \quad \mu(T) = \sum_{i=0}^3 b_i T^i \quad (1)$$

Here, viscosity ( $\mu$ ),  $a$  &  $b$  are constant values, thermal conductivity coefficient ( $\lambda$ ) and  $T$  is the chamber temperature. For the thermo chemical simulation of combustion a polynomial is adopted only for the gas phase and the method of least squares coefficients  $a$  &  $b$  and the mixed local density and the mixture law was used for its computation ((Benarous, et al., 2007). In references Takase (1996) and also according to descriptions in Cutrone et al. (2006) and Wilcox (1998), the standard k-1 two-equation model has been used to simulate turbulent heat transfer with Reynolds Averaged Navier–Stokes (RANS) in a limited channel, in the homogeneous phase model, the written in form of Favre average were solved. Chamber inlet turbulent kinetic energy ( $k$ ) for each flow is as follows:

$$k_{f,ox} = 0.00375 U_{f,ox} U^2 \quad (2)$$

Fuel input rate or oxidizer ( $U_{f,ox}$ ), and ( $u^2$ ) is average square velocity. The two-equation model ( $k$ - $\epsilon$ ) was used with Pop Correction. Using this method, the dynamic behavior of the downstream non-rotating flow of a single injector element is properly expressed.

Table 1: performance conditions of fuel

Performance conditions	H <sub>2</sub>	O <sub>2</sub>
Pressure	6	6
Temperature	287	100
Mass flux	0.07	0.1
Turbulent kinetic energy	381	178

Combustible the gas flow equations include the mass conservation equation, momentum, energy conservation and molecular components transfer equation where for (NR) preliminary reactions are as follows (Majidi Parsa, 2010).

$$\frac{\partial}{\partial t}(\rho A) + \frac{\partial}{\partial x}(\rho u A) = 0 \quad , \quad \frac{\partial}{\partial t}(\rho u A) + \frac{\partial}{\partial x}[(\rho u^2 + p)A] = p \frac{dA}{dx} + F' \quad (3)$$

$$\frac{\partial}{\partial t}(\rho E A) + \frac{\partial}{\partial x}[(\rho u E + u p)A] = \frac{\partial}{\partial x}(q_x A) + q' \quad (4)$$

$$\frac{\partial}{\partial t}(\rho Y_i A) + \frac{\partial}{\partial x}(u p Y_i A) = A \dot{\omega}_i - \frac{\partial}{\partial x}(p \tilde{u}_i Y_i A) \quad (5)$$

$$q_x = \lambda \frac{\partial T}{\partial x} - \rho \sum_{i=1}^{N_s} h_i Y_i \tilde{u}_i \quad , \quad F' = -\frac{\pi}{8} f_g \rho u |u| D \quad , \quad q' = A'_{wh} (q''_h + q''_r) \quad (6)$$

Enthalpy of reaction equation:

$$\frac{\partial \rho h_t}{\partial t} + \frac{\partial \rho u_j h_t}{\partial x_j} = \frac{\partial \rho}{\partial t} + \frac{\partial}{\partial x_j} \left( \rho k \frac{\partial h_t}{\partial x_j} + u_i \tau_{ij} \right) + u_j F_j \quad h_t = h + u_i u_i / 2 \quad (7)$$

Mass fraction of component equation:

$$\frac{\partial [\rho Y_k]}{\partial t} + \frac{\partial}{\partial x_i} [\rho Y_k u_i] = \frac{\partial}{\partial x_i} \left[ \rho D_k \frac{\partial Y_k}{\partial x_i} \right] + \dot{W}_k \quad (8)$$

Mixed reaction model:

$$R_1 = v' M_i A \rho \frac{\varepsilon}{k} \left[ \frac{Y_R}{v'_R M_R} \right] \quad , \quad R_2 = v'_i M_i A \cdot B \rho \frac{\varepsilon}{k} \frac{\sum Y_P}{\sum v'_j M_j} \quad , \quad \dot{W}_k = \text{Min}(R_1, R_2) \quad (9)$$

Eddy dissipation model:

This model is based on eddy breakdown. The turbulence current is formed from a wide range eddy these eddy consume energy in form of friction and their vanishing process leads to shrinking of the eddy. Finally, they vanish and oxygen and hydrogen enter through separate eddy into the combustion chamber. Eddies are broken and get smaller and are stopped and mixed because of friction.

Turbulence model:

For modeling frictional -eddy current, two equations of standard (k-ε) and (RNG) are used. In this model, two values k and ε are computed via two differential equations. Algebraic stress model, in addition to solving the transport differential equations for k and ε, for obtaining each of the Reynolds stress solves an algebraic equation.

$$\frac{\partial}{\partial t}(\rho k) + \frac{\partial}{\partial x_j}(\rho k u_j) = \frac{\partial}{\partial t} \left[ \left( \mu + \frac{\mu_t}{\sigma_k} \right) \frac{\partial k}{\partial x_j} \right] + G_k - \rho \varepsilon \quad (10)$$

$$\frac{\partial}{\partial t}(\rho \varepsilon) + \frac{\partial}{\partial x_j}(\rho \varepsilon u_j) = \frac{\partial}{\partial t} \left[ \left( \mu + \frac{\mu_t}{\sigma_\varepsilon} \right) \frac{\partial \varepsilon}{\partial x_j} \right] + C_1 \frac{\varepsilon}{k} (G_k) - C_2 \rho \frac{\varepsilon^2}{k} - R_\varepsilon$$

$$\mu_t = C_\mu \rho \frac{k^2}{\varepsilon} \quad (11)$$

Here,  $q_x$  is thermal conductivity in gases and thermal effects due to the influence of components mass,  $F'$  is frictional drag of chamber,  $q'$  is the effects of heat transfer to wall includes displacement heat flux, are modeled as below (Zhang, et al., 2007)  $q''_r$  and radiant heat flux  $q''_h$

$$q''_h = h_g (T_{wh} - T_{aw}) \quad , \quad q''_r = \varepsilon_g \sigma (T_{wh}^4 - T_g^4) \quad (12)$$

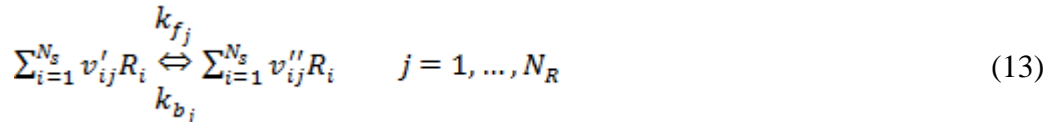
Where,

P, u, and T<sub>g</sub> are pressure, velocity and temperature of gas, E is specific total energy, A is sectional area of flow,  $h_{f_i}^0$

is formation enthalpy of component i, λ is thermal conductivity coefficient of gas,  $h_i$  specific enthalpy of component i, ρ is gas density,  $\tilde{u}_i$  is infiltration rate of component i,  $Y_i$  is mass fraction of component i,  $f_g$  is

Darcy friction factor,  $D$  is hydraulic diameter of the chamber,  $A'_{wh}$  is gas -side wall surface area per unit length  $x$ ,  $h_g$  is coefficient of heat transfer of gas,  $T_{wh}$  is gas-side wall temperature,  $\sigma$ , the Stefan - Boltzmann constant,  $\epsilon_g$  gas presidents coefficient,  $T_{aw}$  adiabatic wall temperature (Zhang, et al., 2007).

The subtitles  $i$  and  $N_s$  show each component and total number of chemical constituents. To determine the friction coefficient value, the Colebrook equation (Fox & McDonald, 1994) and for determination of the heat transfer coefficient between the gas and the wall, the Bartz equation (Zhang, et al., 2007) were applied. The used chemical model is the combustion air - hydrogen model containing 9 components and 18 preliminary reactions (VanOverbeke and Shuen, 1989). For  $N_R$  the preliminary reaction could be written as:



Where,

$R_i v'_{ij}$  and  $v''_{ij}$  are symbol of component  $i$ , the Stoichiometric coefficient of component  $i$  irrespectively which are reciprocating in reaction  $j$ .  $k_{f_j}$  And  $k_{b_j}$  are constant rate of reciprocating  $j$  reaction which are a function of temperature and gas are determined by the Arrhenius equation.

$$k_{f_j} = A_{f_j} T^{B_{f_j}} e^{-E_{f_j}/RT} \quad , \quad k_{b_j} = A_{b_j} T^{B_{b_j}} e^{-E_{b_j}/RT} \quad (14)$$

Where,

Free energy of reaction  $E_{f_j}$  and  $E_{b_j}$  are energy of releasing sweep  $j$  reaction,  $A_{f_j}$ ,  $B_{f_j}$ ,  $A_{b_j}$  and  $B_{b_j}$  are constants sweep  $j$  reaction. Rate of change of molar concentration of component  $j$ th by reaction  $j$ th is  $(\dot{C}_i)_j$  which  $\dot{C}_i$  concentration of component  $j$  is. The overall changing rate of mass concentration of component  $(\dot{\omega}_i)$  is written as below:

$$(\dot{C}_i)_j = (v''_{ij} - v'_{ij}) \left[ k_{f_j} \prod_{l=1}^{N_s} C_l^{v'_{lj}} - k_{b_j} \prod_{l=1}^{N_s} C_l^{v''_{lj}} \right] \quad , \quad \dot{\omega}_i = \sum_{j=1}^{N_R} M_i (\dot{C}_i)_j \quad (15)$$

Specific heat at constant pressure, thermal conductivity and viscosity of each chemical component is determined with a polynomial of degree four (VanOverbeke and Shuen, 1989).

The assumption of quasi-one-dimensional flow was used to simulate the fluid passing through the cooling channel.

In this study, cooling fluid with specific mass flow passes from nozzle end through injection channel and flows in opposite direction of passing gas flow in the chamber. The equations consist of continuity equations; momentum size and energy assuming refrigerant density in form of polynomial degree two in terms of fluid temperature are as follows respectively (Marchi, et al., 2004):

$$\frac{d}{ds} (\rho_c u_c A) = 0 \quad , \quad \frac{d}{ds} (\rho_c u_c^2 A) = -A \frac{d\rho_c}{ds} + F' \quad (16)$$

$$c_{p_c} \frac{d}{ds} (\rho_c u_c A T_c) = \beta T_c u_c A \frac{d\rho_c}{ds} + q' \quad , \quad \rho_c = \rho + \rho_2 T_c + \rho_3 T_c^2 \quad (17)$$

In these equations,  $F'$  is channel friction drag,  $q'$  includes two works of friction and heat transfer between the walls and is written as below:

$$F' = -\frac{\pi}{8} f_c \rho_c u_c |u_c| D \quad , \quad q' = |u_c F'| + A'_{wc} q''_c \quad , \quad q''_c = h_c (T_{wc} - T_c) \quad (18)$$

In the above relation ,  $P_c$  ,  $u_c$  ,  $\rho_c$  and  $T_c$  are used for density, velocity, pressure and temperature of the cooling fluid, S the direction of the flow in channel, A cross-sectional area of the fluid in the channel,  $C_{pc}$  specific heat at constant pressure of the cooling fluid,  $\beta$  the volumetric thermal expansion coefficient, and  $f_c$  and D Darcy friction coefficient and hydraulic diameter of the channel respectively,  $A_{w,c}$  thermal transfer between the cooling fluid and  $A'_{w,c}$  represents  $A_{w,c}$  onto the unit of length s,  $q_c''$  heat flux,  $h_c$  heat transfer coefficient between the cooling fluid and the wall and  $T_{w,c}$  wall temperature of the refrigerant and for solving the equations , the implicit method is extended for combustible flows , were applied for solving the equations for the gas flow.

### Simulation results:

In following, the output results of temperature counters in the combustion chamber of engine from the simulation software are presented.

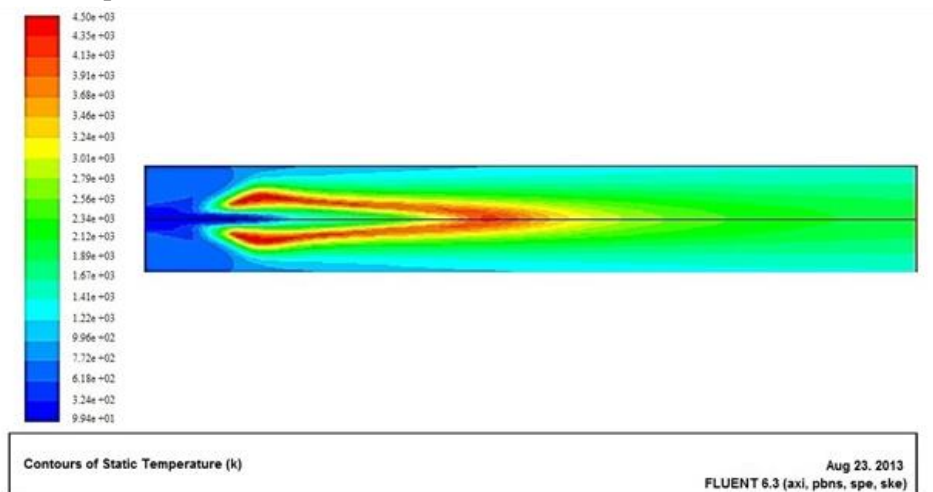


Fig.5: Static temperatures counter in engine combustion chamber

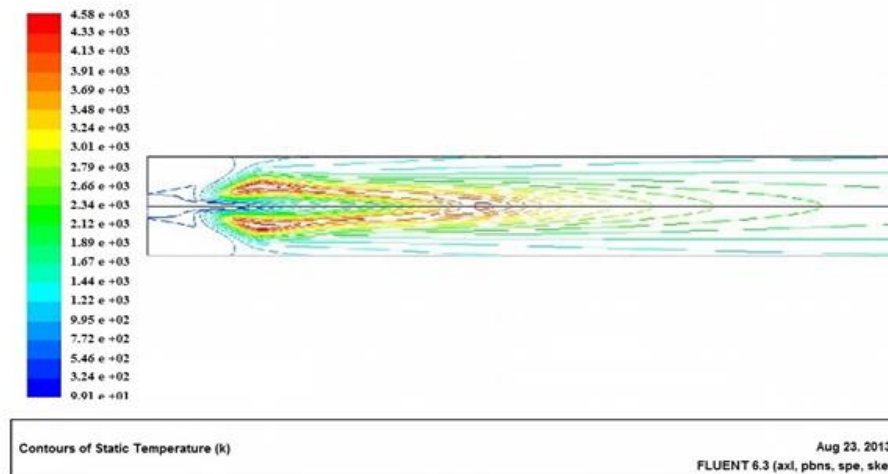


Fig.6: Isothermal contours of static temperature combustion chamber

Combustion temperature in the central part of the screen to the injector changes as: first in the injector inlet to the chamber, since no collision has not lead to sustainable combustion yet, combustion occurs very low and in the boundary layer between two flow directions. The initial temperature is average of two injected jet temperature into the chamber and approximately 100k. After jet collision and initiation of mixing and combustion, temperature will rise, but the reaction has not reached the required temperature to the highest

possible speed. Treatment yet not led to sustained ignition combustion is very low and the boundary layer between the jet stream occurs.

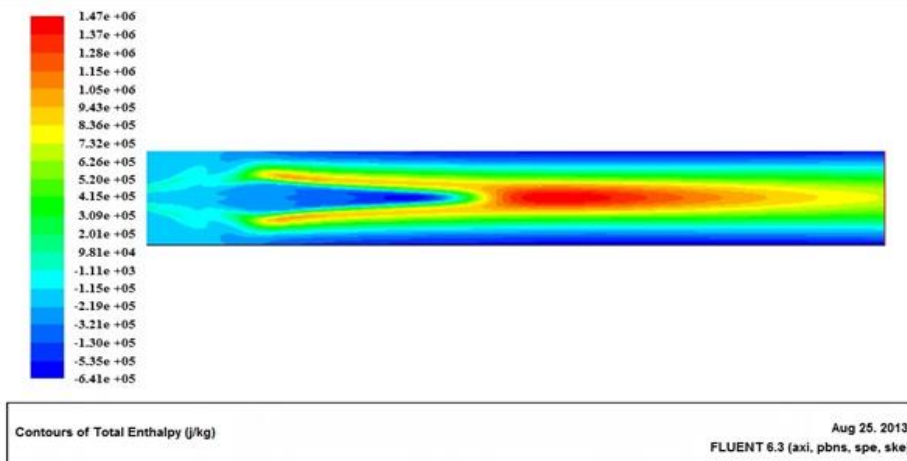


Fig.7: Contour of the reaction enthalpy of combustion chamber

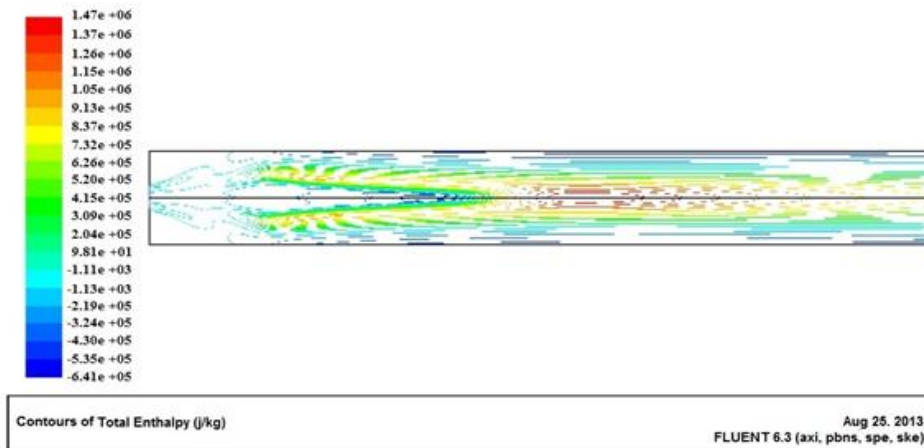


Fig.8: lines with same enthalpy flow over the combustion chamber

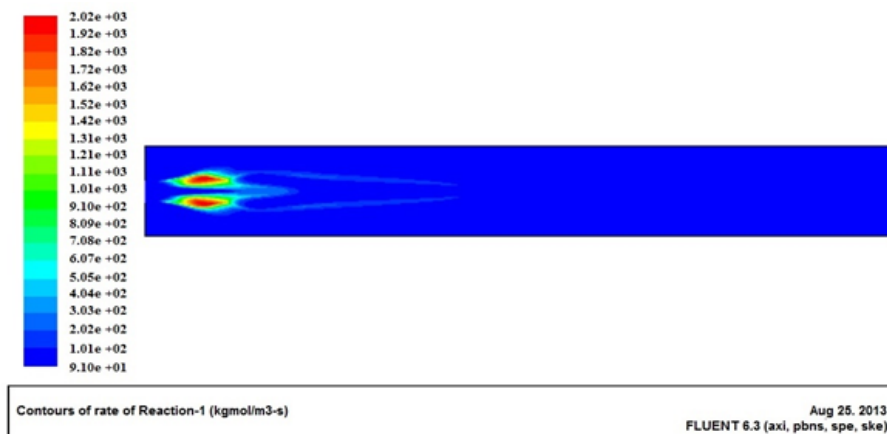


Fig.9: Contour reaction rate turbulent of combustion engine

From 100mm distance the injector goes to completion due to formation of large eddy and temperature increases rapidly due to the formation of hot product again, until it reaches its maximum value over the chamber. After this distance, the reaction reaches equilibrium and the maximum temperature of combustion,



mixes with remaining temperature of hydrogen fuel jet with 298k temperature. The temperature begins to decrease and eventually reaches a relatively uniform balance temperature and leads to about 2400k on motor output.

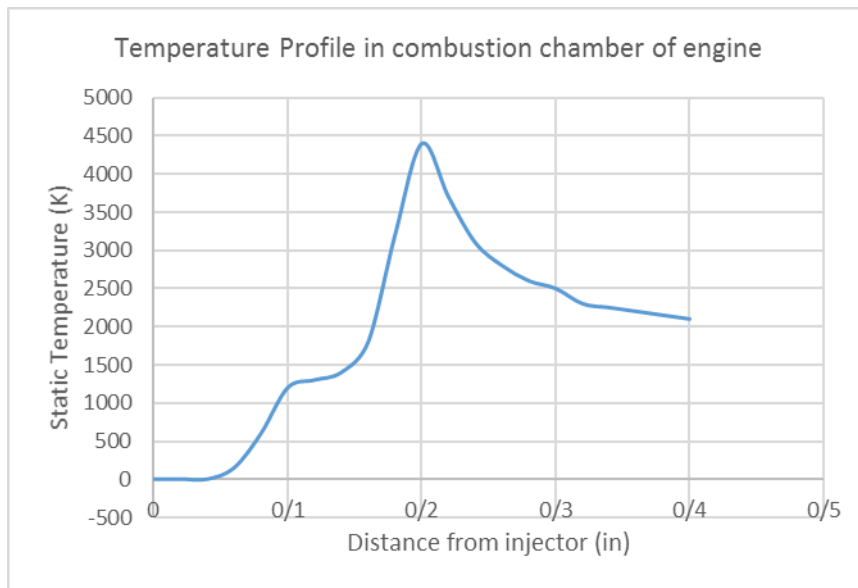


Fig.10: temperature profile in combustion chamber of engine

Comparison of the above and below diagrams indicates that combustion model used in simulation shows properly the temperature of combustion with a difference near 200K. Simulation revealed that combustion chamber temperature shows a rapid increase in 0.1mm distance and reaches its maximum rate, i.e. 1900K, and combustion gases exit from the chamber with an average temperature of 1900K. As figures 5 and 7 show, the temperature distribution along combustion chamber can be predicted properly by using proper combustion model and the existing method.

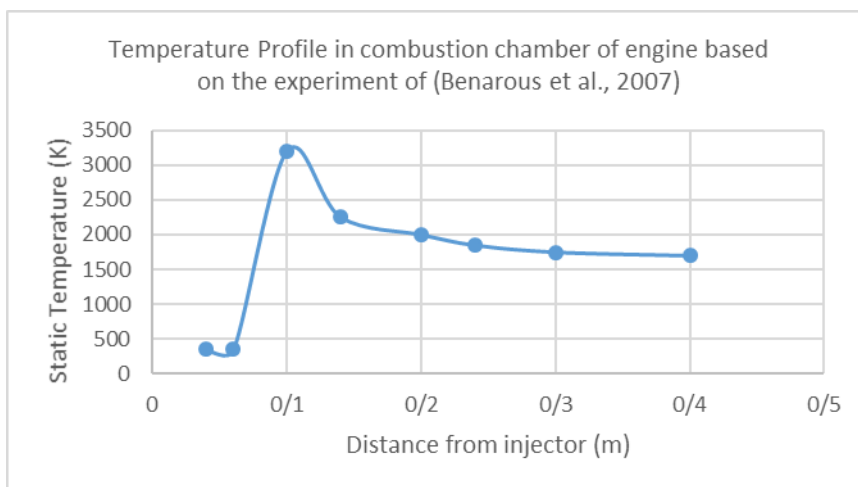


Fig.11: temperature profile in combustion chamber of engine based on the experiment of benarous et al, 2007

The effects of the channel height and the effect of fin thickness and the thickness of the inner wall of the chamber on axial distribution of the wall temperature of the gas-side are shown in Fig.10 & 11.

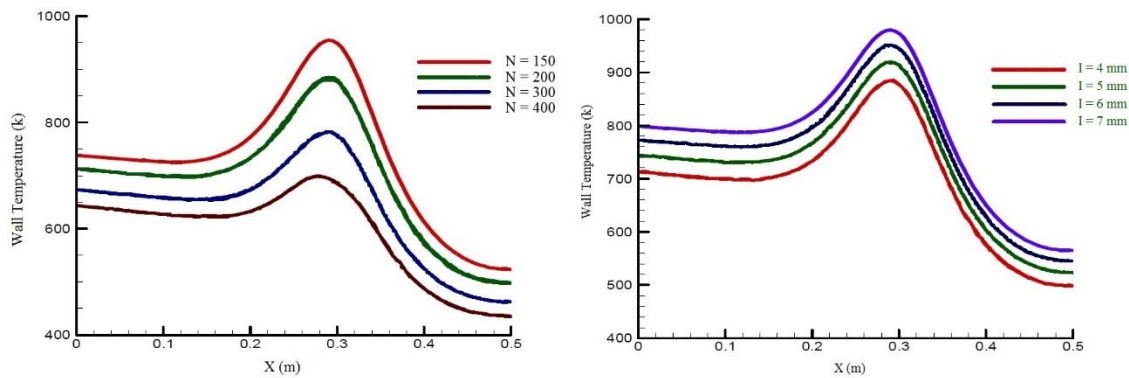


Fig.12: Axial distribution of wall temperature at different number of channels (left) and for different channel height (right)

According to diagram in Fig.10 ( right hand side), it could be said that as channel height increases from 4 to 7, the wall temperature rises to about  $100^{\circ}\text{K}$ . But increasing number of cooling channels, the wall temperature reduces about  $150^{\circ}\text{K}$ .

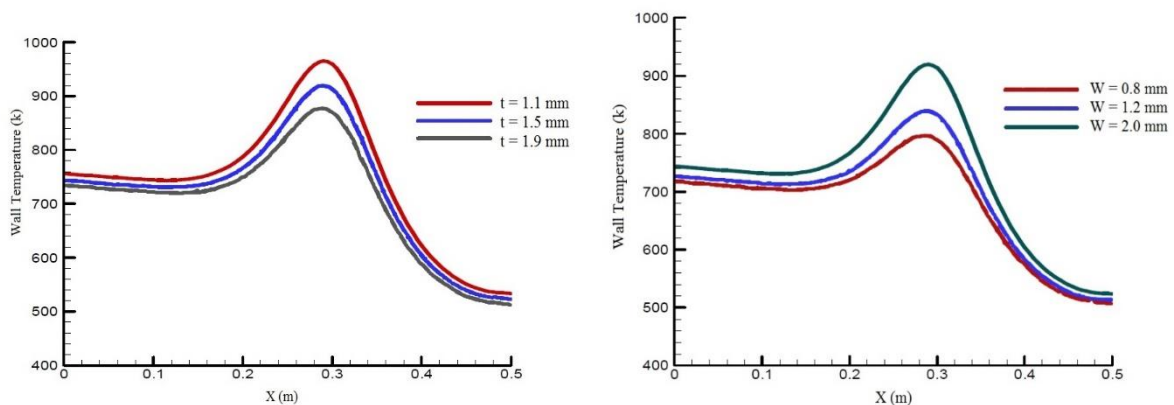


Fig.13: Axial distribution of wall temperature at different thicknesses Finn (left) and different wall thicknesses (right)

Considering the diagram in Fig.11 (right hand side), the right wall temperature will increase with increasing wall thickness. As the diagram shows, this increase is non-linear and highly progressive. Increase of fin thickness causes reduction in the maximum temperature of the wall. Fig.12 and 13 illustrates the effect of changing height and number of channels, Fin thickness and thickness of inner wall on the maximum wall temperature of the gas.

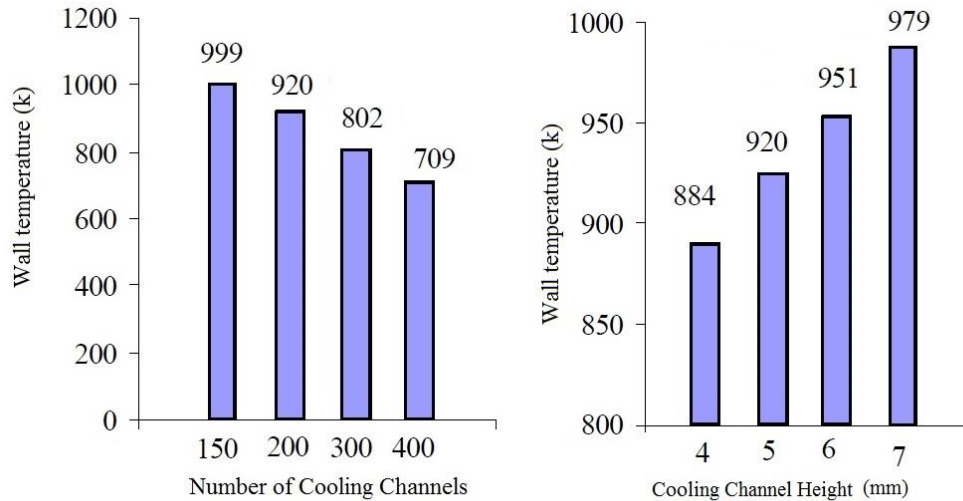


Fig.14: Effect of changes in channel number (left) and channel height (right), the maximum wall temperature

As shown in the above diagram, increasing number of cooling channels has a direct impact on reducing the maximum wall temperature. This reduced temperature is to somewhat close to the curve. About increase of the cooling channels height it can also be said that with increasing height of the wall temperature will increase due to transfer rules is reasonable and expected.

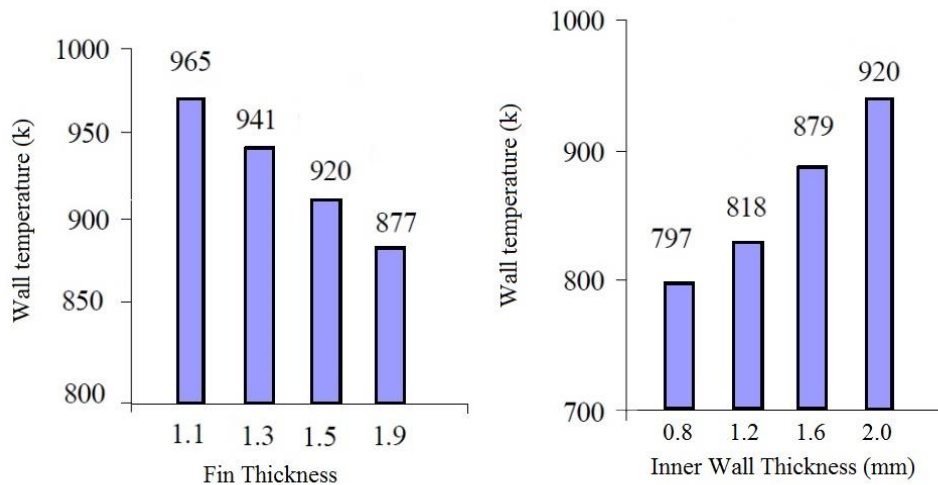


Fig. 15: Evaluation of the effects of fin thickness (left) and the thickness of the inner wall (right), the maximum wall temperature

Diagram 13 shows that with increase of fin thickness, the maximum wall temperature decreases and with increase of inner wall, as the right hand diagram shows, the maximum temperature will increase which because of the heat transfer characteristics of the wall is reasonably expected.

### Conclusion:

The combustion model used in the simulation profile displays well temperature caused by combustion with a difference approximately 200k. In the injector inlet to the chamber, since no collision occurs yet, no sustainable combustion is created and combustion takes place very low and in the boundary layer between to

jets of flows. The initial temperature is an average of two injected jet flows into the chamber and about 100k. After the jets collision and mixing and combustion, temperature shows an increase, but the reaction does not reach the required temperature for reaching the highest speed. From 100mm distance, the mixing injector goes towards completion due to formation of large eddies and temperature because of formation of a hot product increases rapidly to reach the maximum value over the chamber. After this distance, the reaction reaches equilibrium and the maximum temperature caused by combustion, mixes with the temperature of remaining hydrogen fuel jet at 298k and temperature begins to reduce.

Finally, the effect of geometrical parameters of cooling channels on rate of the rate of heat transfer through the cooling channel wall thrust chamber of liquid-fuel engines, the cooling fluid channel and the thermal conductivity of the walls were studied. For effective cooling thrust chamber, the wall temperature of the hot gases must be lower than the melting temperature of wall. This can be done by increasing the cooling fluid flow, reduction of cross-sectional area of the fluid passing through the cooling channels by reducing channel height and fin thickness, sex change and reduction of the thickness of the inner wall of the engine.

### References:

- Benarous, A., Liazid, A., Karmed, D., 2007. "H<sub>2</sub>O<sub>2</sub> Combustion under supercritical Conditions" Third European Combustion Meeting ECM .
- Cai, G., Fang, J., Xu, X. and Liu, M., Performance Prediction and Optimization for Liquid Rocket Engine Nozzle, *Aerospace Science and Technology*, 2007, pp. 155–162 .
- Candel, S. Herding, G. Scoufflaire, P. Rolon, C. Vingert, L. Habiballah, M. Grisch, F. Pealat, M. Bouchardy, P. Stepowsky, D. Cessou, A. Colin, P. 1998. "Experimental investigation of shear coaxial cryogenic jet flames", *Journal of Propulsion and Power* 14 pp. 826–834.
- Chehroudi, Talley, D. and Coy, E. 2002. "Visual characteristics and initial growth rates of round cryogenic jets at subcritical and supercritical pressures," *Phys. Fluids* 14, pp. 850.
- Cutrone, L. Ihme, M. Herrmann, 2006. M. "Modeling of high-pressure mixing and combustion in liquid rocket injectors", *Center for Turbulence Research Proceedings of the Summer Program*.
- Daimon, H. Negishi, H. Kawashima, Conjugated combustion and heat transfer simulations of upper and lower main combustion chambers of LE-9 engine, in: *AIAA paper 2019-4112*, 2019,
- Fox, R.W., and McDonald, A.T., *Introduction to Fluid Mechanics*, 4th Ed., John Wiley&sons, New York, 1994 .
- Gutheil, E.; 2001 "Turbulent Spray Combustion Modeling for Rocket Engine Applications" 2nd International Workshop on Rocket Combustion Modeling: Atomization, Combustion and Heat Transfer held in Lampoldshausen, Germany.
- Jin Y., Xu X., Yang Q., Zhu S, Numerical investigation of flame appearance and heat flux and in a deep-throttling variable thrust rocket engine, *Aerosp. Sci. Technol.*, 88 (2019), pp. 457-467, 10.1016/j.ast.2019.03.042
- Leccese G., Bianchi D., Betti B., Lentini D., Nasuti F, Convective and radiative wall heat transfer in liquid rocket thrust chambers, *J. Propul. Power*, 34 (2) (2018), pp. 318-326, 10.2514/1.B36589
- M. Frey, T. Aichner, J. Görden, B. Ivancic, B. Kniesner, O. Knab, Modeling of rocket combustion devices, in: *AIAA paper 2010-4329*, 2010, <http://dx.doi.org/10.2514/6.2010-4329>.
- Majdi Parsa, M. (2010). Modeling fluid flow and heat transfer in the thrust combustion chamber of fluid fuel of retrieval cooling, Master's dissertation, Khajeh Nasir Tousi University.
- Marchi, C.H., Laroca, F., Da Silva, A.C., Hinckel, J.N., Numerical Solutions of Flows in Rocket Engines with Regenerative Cooling, *Numerical Heat Transfer*, Vol. 45, 2004. pp. 699–717.
- Masquelet M.M., 2006. "Simulations of a Sub-scale Liquid Rocket Engine Transient Heat Transfer in a Real Gas Environment" Master-thesis, Aerospace Engineering Georgia Institute of Technology .
- Mayer, W. Tamura, H. 1996. "Propellant injection in a liquid oxygen/gaseous hydrogen rocket engine", *Journal of Propulsion and Power* 12 (6) pp. 1137–1147.

- Mayer, W. Telaar, R.J. Branam, J. Hussong, J. 2003. "Raman measurements of cryogenic injection at supercritical pressure", *Heat and Mass Transfer* 39 709–719.
- Nureddin Dinler, and Nuri Yucel; 2007 "Numerical Simulation of Flow and Combustion in an Axisymmetric Internal Combustion Engine" *World Academy of Science, Engineering and Technology*, vol. 36.
- Oschwald M. and Schik, A. 1999. "Supercritical nitrogen free jet investigated by spontaneous Raman scattering," *Exp. Fluids* 27, 497, 497–506.
- Oschwald, M. Smith, J.J. Branam, R. Hussong, J. Schik, A. Chehroudi, B. Talley, D. 2006. "Injection of supercritical fluids into supercritical environment", *Combustion Science and Technology* 178 (1–3) pp. 49–100.
- Reddy, S. K., Pandey K. M., and Singh, A. P., 2011 "Numerical Simulation with K-E Turbulence Model for Combustion Chamber of Rocket Engines" *The 11th Asian International Conference on Fluid Machinery and Paper number 220 The 3rd Fluid Power Technology Exhibition, IIT Madras, Chennai, India.*
- Smith, J. Klimenko, D. Clauss, W. Mayer, W. 2002. "Supercritical LOX/Hydrogen Rocket Combustion Investigations Using Optical Diagnostics", Paper AIAA-2002-4033, 38th AIAA/ASME/SAE/ASEE Joint Propulsion Conference & Exhibit, Indianapolis.
- Song J., Sun B, Coupled numerical simulation of combustion and regenerative cooling in LOX/methane rocket engines, *Appl. Therm. Eng.*, 106 (2016), pp. 762-773, 10.1016/j.applthermaleng.2016.05.130
- Takase, K. 1996, "Numerical prediction of augmented turbulent heat transfer in an annular fuel channel with repeated two-dimensional square ribs", *Nuclear Engineering and Design*, Vol. 165 Nos 1/2, pp. 225-37.
- VanOverbeke, T.J., Shuen, J.S, A Numerical Study of Chemically Reacting Flow in Nozzles, AIAA-89-2793, 1989.
- Veynante, D., Vervisch, L. 2002 "Turbulent combustion modeling" *Progress in Energy and Combustion Science* 28 193-266 .
- Wang, Q., Wu, F., Zeng, M., Luo, L., Sun, J., 2006. "Numerical Simulation and Optimization on Heat Transfer and Fluid Flow in Cooling Channel of Liquid Rocket Engine Thrust Chamber", *Numerical Simulation and Optimization*, pp. 907-921 .
- Wilcox, D. C. 1998. *Turbulence Models for CFD*. DCW Industries, Inc.
- Xu J., Jin P., Li R., Wang J., Cai G, Effect of coaxial injector parameters on LOX/methane engines: A numerical analysis, *Acta Astronaut.*, 171 (2020), pp. 225-237, 10.1016/j.actaastro.2020.02.055
- Zhang, H.W., He, Y.L., Tao, W.Q., Numerical Study of Film and Regenerative Cooling in a Thrust Chamber at High Pressure, *Numerical Heat Transfer*, 2007, pp. 991–1007 .